



## Structure–selectivity relationship of a zirconia-based heterogeneous acid catalyst in the production of green mono- and dioleate product

Pei San Kong, Yolande Peres-Lucchese, Patrick Cognet, François Senocq, Wan Mohd Ashri Wan Daud, Mohamed Kheireddine Aroua, Haniza Ahmad, Revathy Sankaran, Pau Loke Show

### ► To cite this version:

Pei San Kong, Yolande Peres-Lucchese, Patrick Cognet, François Senocq, Wan Mohd Ashri Wan Daud, et al.. Structure–selectivity relationship of a zirconia-based heterogeneous acid catalyst in the production of green mono- and dioleate product. *Clean Technologies and Environmental Policy*, 2020, pp.0. 10.1007/s10098-020-01830-1 . hal-02651368

**HAL Id: hal-02651368**

**<https://hal.science/hal-02651368>**

Submitted on 29 May 2020

**HAL** is a multi-disciplinary open access archive for the deposit and dissemination of scientific research documents, whether they are published or not. The documents may come from teaching and research institutions in France or abroad, or from public or private research centers.

L'archive ouverte pluridisciplinaire **HAL**, est destinée au dépôt et à la diffusion de documents scientifiques de niveau recherche, publiés ou non, émanant des établissements d'enseignement et de recherche français ou étrangers, des laboratoires publics ou privés.



## Open Archive Toulouse Archive Ouverte



OATAO is an open access repository that collects the work of Toulouse researchers and makes it freely available over the web where possible

This is an author's version published in: <http://oatao.univ-toulouse.fr/25852>

### Official URL:

<https://doi.org/10.1007/s10098-020-01830-1>

### To cite this version:

Kong, Pei San and Peres-Lucchese, Yolande  and Cognet, Patrick  and Senocq, François and Daud, Wan Mohd Ashri Wan and Aroua, Mohamed Kheireddine and Ahmad, Haniza and Sankaran, Revathy and Show, Pau Loke *Structure–selectivity relationship of a zirconia-based heterogeneous acid catalyst in the production of green mono- and dioleate product.* (2020) Clean Technologies and Environmental Policy. ISSN 1618-954X.

Any correspondence concerning this service should be sent to the repository administrator: [tech-oatao@listes-diff.inp-toulouse.fr](mailto:tech-oatao@listes-diff.inp-toulouse.fr)

# Structure–selectivity relationship of a zirconia-based heterogeneous acid catalyst in the production of green mono- and dioleate product

Pei San Kong<sup>1</sup> · Yolande Pérès<sup>2</sup> · Patrick Cognet<sup>2</sup> · François Senocq<sup>3</sup> · Wan Mohd Ashri Wan Daud<sup>4</sup> · Mohamed Kheireddine Aroua<sup>5,6</sup> · Haniza Ahmad<sup>1</sup> · Revathy Sankaran<sup>7</sup> · Pau Loke Show<sup>8</sup>

## Abstract

A novel catalytic technique is vital to produce mono- and dioleate (GMO and GDO) from bioglycerol: a renewable resource and by-product of biodiesel. The advantage of this invention is the direct production of GMO and GDO through catalytic approach compared to the conventional method that requires transesterification and distillation processes. In this paper, glycerol esterification with oleic acid using a catalyst was experimented. The process was carried out over a hydrophobic mesoporous zirconia–silica heterogeneous acid catalyst ( $\text{ZrO}_2\text{–SiO}_2\text{–Me\&Et–PhSO}_3\text{H}$ ) with three types of sulphated zirconia catalysts ( $\text{SO}_4^{2-}/\text{ZrO}_2$ ) to produce high-selectivity GMO and GDO products. The catalytic performance of the hydrophobic  $\text{ZrO}_2\text{–SiO}_2\text{–Me\&Et–PhSO}_3\text{H}$  catalyst was benchmarked with that of  $\text{SO}_4^{2-}/\text{ZrO}_2$  which was developed from three zirconium precursors. Results showed that the pore volume and hydrophobicity of the designed catalyst greatly could influence the product selectivity, thus enabling smaller substrates GMO and GDO to be dominated in the synthesis. This finding was supported by characterisation data obtained through  $\text{N}_2$  adsorption–desorption, X-ray diffraction and scanning electron microscopy. In addition, a good correlation was found between pore volume (pore size) and product selectivity. High pore volume catalyst favoured GDO production under identical reaction conditions. Pore volume and size can be used to control product sensitivity. The hydrophobicity of the catalyst was found to improve the initial reaction rate effectively.

✉ Pei San Kong  
sylvia.kong.peisan@simedarbyplantation.com

✉ Mohamed Kheireddine Aroua  
kheireddinea@sunway.edu.my

Sime Darby Plantation Research Sdn. Bhd. (Formerly Known as Sime Darby Research Sdn. Bhd.), Lot 2664, Jalan Pulau Carey, 42960 Pulau Carey, Selangor Darul Ehsan, Malaysia

<sup>2</sup> Laboratoire de Génie Chimique, CNRS, INP, UPS, Université de Toulouse, Toulouse, France

CIRIMAT, CNRS, INPT, UPS, Université de Toulouse, Toulouse, France

<sup>4</sup> Department of Chemical Engineering, Faculty of Engineering, University of Malaya, 50603 Kuala Lumpur, Malaysia

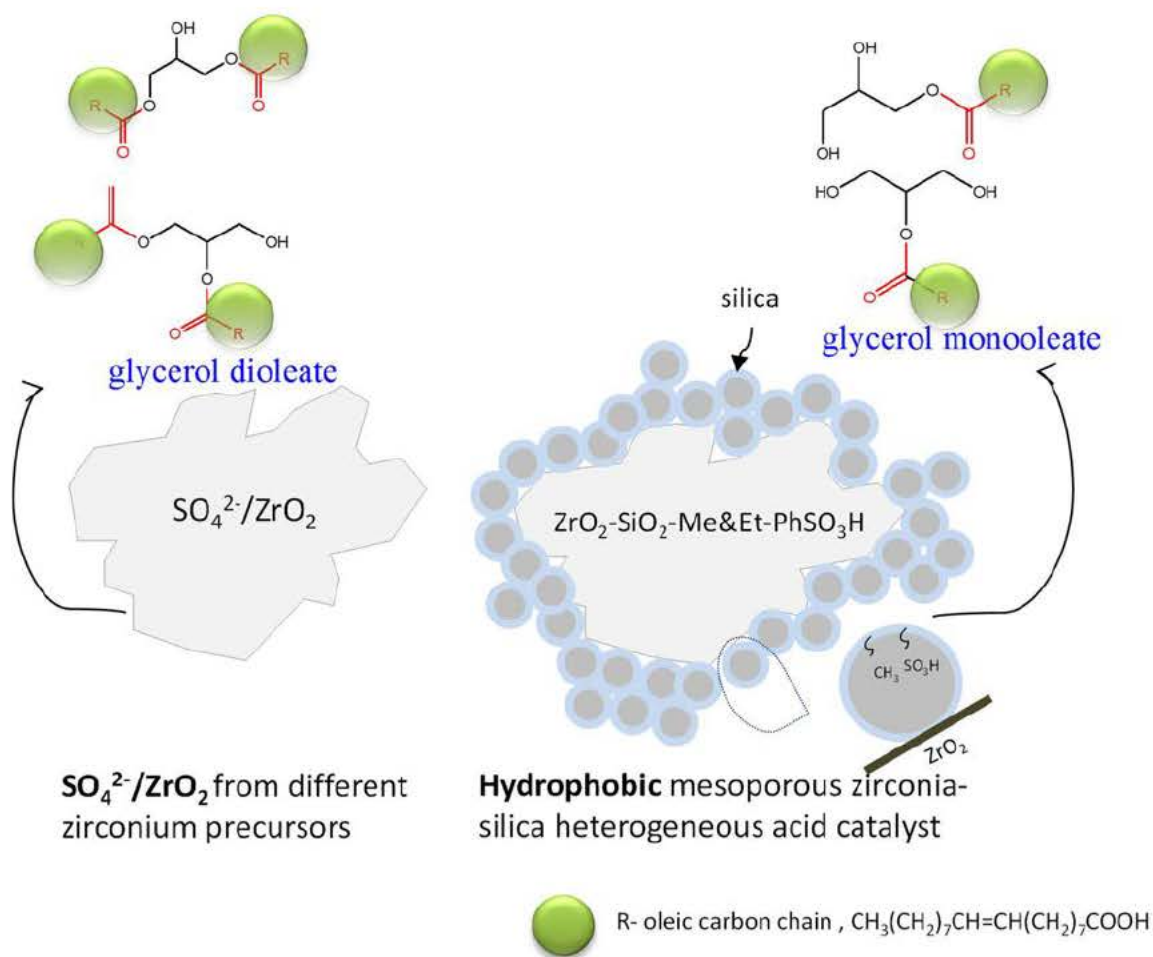
Centre for Carbon Dioxide Capture and Utilization (CCDCU), School of Science and Technology, Sunway University, 47500 Bandar Sunway, Selangor Darul Ehsan, Malaysia

Department of Engineering, Lancaster University, Lancaster LA1 4YW, UK

<sup>7</sup> Institute of Biological Sciences, Faculty of Science, University of Malaya, 50603 Kuala Lumpur, Malaysia

Department of Chemical and Environmental Engineering, Faculty of Science and Engineering, University of Nottingham Malaysia, Jalan Broga, 43500 Semenyih, Selangor Darul Ehsan, Malaysia

## Graphical abstract



**Keywords** Hydrophobic silica–zirconia-based catalyst · Sulphated zirconia · Structural · Selectivity · Esterification · Glycerol

## Introduction

Recently, the research on glycerol conversion to high-value chemicals is gaining much attention due to the abundant glycerol production and its undeniably low value (Kong et al. 2016; Quispe et al. 2013). The acid catalytic system is generally applied in several processes such as esterification, etherification, polymerisation, dehydration, acetylation or glycosylation (Kong et al. 2015, 2016b, Karam et al. 2017). Esterification of glycerol with large-size oleic acid (OA) molecule in the presence of catalyst is able to yield many high-value-added chemicals such as glycerol monostearate, glyceryl dioleate and glyceryl trioleate. Nevertheless, designing a heterogeneous acid catalyst for the catalytic transformation of glycerol into value-added derivatives is challenging because of the difficult

accessibility of glycerol catalytic sites and because of the impact of complex structural properties on product selectivity (Jérôme et al. 2008). In addition, recent studies have shown that hydrophobic catalyst surface is crucial to strengthen the polar glycerol activity reaction and immiscible reactants (Estevez et al. 2016; Gaudin et al. 2011; Konwar et al. 2016).

GMO and GDO are classified as lipids, and they have several unique properties such as amphiphilic nature, non-ionic and great emulsifier. They are extensively utilised in various industries such as food, cosmetic and pharmaceutical industries, and they are also employed in aqueous fibre finishing (Macierzanka and Szeląg 2004; Thengumpillil et al. 2002). At different operating conditions such as varying temperatures and diverse solvent composition, the GMO is able to reconstruct into distinct crystalline

structures due to its amphiphilic nature (Kulkarni et al. 2011). The robust expanding industries such as nutraceuticals, pharmaceuticals and lubricants are the major channels for GMO. In the health care industry, it is reported that GMOs and GDO are considered as appealing lipids for the formulation of potential vehicles of drugs and to improve the poor solubilisation of bioactive compounds. GMO and GDO lipids could enhance their bio-accessibility at intestinal level or to protect against their degradation under gastrointestinal conditions, which eventually achieve the most efficient bioactivity compounds in a self-emulsifying lipid delivery system. The need for GMOs is associated with the requirement from the health care or lubricant market owing to the slow market of food and plastics industries (Frost and Sullivan Research Service 2014). At the moment, GDO is widely employed in drug delivery and applied as a safe plasticiser in the polymer industry (Barauskas et al. 2006; Zhang et al. 2017).

To date, heterogeneous acid catalysts, such as ion exchange resins (Åkerman et al. 2011), zeolites (Singh et al. 2013), double-metal cyanide complexes (Kotwal et al. 2011), heteropolyacid-supported catalysts (Wee et al. 2013), hydrotalcite (Hamerski and Corazza 2014; Hamerski et al. 2016) and sulphated metal oxide catalysts (Kong et al. 2015), have been explored for catalytic glycerol esterification with OA. On the contrary, the drawbacks of homogeneous acid catalysts are dark product colour and burnt taste and require additional refining steps. Homogeneous acid catalyst can disperse into the reactants rapidly but resulted in poor product selectivity. In a recent study, it was demonstrated that the application of the Fe–Zn DMC complex is able to achieve GMO conversion with 63.4% and GMO selectivity of 67.3% under optimised conditions of 180 °C reaction temperature, 8 wt.% catalyst loading and 8 h of reaction time (Kotwal et al. 2011). Meanwhile, titanium silicate-type catalyst (Ti-SBA-16) featuring a hydrophobic surface attained a conversion of 72.8% at 180 °C, equimolar ratio, 3 wt % catalyst concentration and 3 h of operation time. The presence of catalyst sites in Ti-SBA-16 catalyst is not the only reason contributing to the excellent catalytic performance, but also the catalyst structure further helps in maximising the selectivity of the anticipated products. It was reported that the hydrophobicity characteristic of Ti metal is able to enhance the glycerol esterification rate and selectivity. However, the high reaction temperature (180 °C) and long reaction time (10 h) are several of the limitations that could be improved to synthesise promising solid acid catalysts.

Therefore, this work aims to examine the relationship of the structural and hydrophobicity surface of a heterogeneous catalyst with the product selectivity over four zirconia-based heterogeneous acid catalysts, for the industrially important glycerol catalyst-assisted esterification with OA. To the best

of our knowledge, this study is the first to provide insights into the impact of pore size, pore volume and hydrophobicity of catalyst surface towards the product selectivity via various zirconia-precursor-developed catalysts. The comparative catalytic activity for the  $\text{ZrO}_2\text{--SiO}_2\text{--Me\&Et--PhSO}_3\text{H}$  catalyst (higher hydrophobicity) with three types of  $\text{SO}_4^{2-}/\text{ZrO}_2$  catalysts [less hydrophobic and developed from different zirconium precursors,  $\text{Zr}(\text{OCH}_2\text{CH}_3)_4$ ,  $\text{ZrOCl}_2\cdot 8\text{H}_2\text{O}$  and commercial  $\text{Zr}(\text{OH})_4$ ] was investigated. The catalyst synthetic methods for  $\text{SO}_4^{2-}/\text{ZrO}_{2\text{sol-gel}}$ ,  $\text{SO}_4^{2-}/\text{ZrO}_{2\text{precipitation}}$ ,  $\text{SO}_4^{2-}/\text{ZrO}_{2\text{commercial}}$  and highly hydrophobic  $\text{ZrO}_2\text{--SiO}_2\text{--Me\&Et--PhSO}_3\text{H}$  and their textural properties were characterised. The esterification reactions are performed at a steady amount of acidity, and the reaction conditions are optimised to assess the effect of the textural properties on catalytic performance.

## Experimental

### Materials

The chemicals used in this study are similar to our previous paper (Kong et al. 2018). For the synthesis of  $\text{ZrO}_2\text{--SiO}_2\text{--Me\&Et--PhSO}_3\text{H}$  hydrophobic-enhanced catalyst, chemicals utilised are zirconium hydroxide powder, ethanol, ammonia solution (25%), tetraethyl orthosilicate, trimethoxymethylsilane (TMMS) and dry toluene that were obtained from Sigma-Aldrich. 2-(4-chlorosulphonylphenyl) ethyltrimethoxysilane (CSPETS, 50% in dichloromethane and sulphuric acid solution ( $\text{H}_2\text{SO}_4$ , 99.99%)) were obtained from Fisher Scientific. Other chemicals that include zirconium (IV) propoxide,  $\text{Zr}(\text{OCH}_2\text{CH}_2\text{CH}_3)_4$  precursor, 1-propanol and 0.5 M aqueous  $\text{H}_2\text{SO}_4$  were obtained from Sigma-Aldrich. These chemicals are used to create sol-gel method-prepared catalyst ( $\text{SO}_4^{2-}/\text{ZrO}_{2\text{sol-gel}}$ ). As for the ( $\text{SO}_4^{2-}/\text{ZrO}_{2\text{precipitation}}$ ) catalyst synthesis, the materials can be found in the paper (Kong et al. 2018). Reactants glycerol and technical grade OA were acquired from Sigma-Aldrich. Monoolein, diolein and triolein that were used for quantitatively product analysis were obtained from Sigma-Aldrich. Analytical-grade solvents purchased from Sigma-Aldrich, such as acetonitrile (ACN), methanol (MeOH) and tetrahydrofuran (THF), were used as the mobile phase. Trifluoroacetic acid (TFA) was used as a mobile phase additive due to its high resolving power.

### Catalyst preparations

A catalyst featuring hydrophobic surface was synthesised by using modified volume of TMMS hydrophobic agent



(ZrO<sub>2</sub>-SiO<sub>2</sub>-Me&Et-PhSO<sub>3</sub>H) as described in the previous study (Kong et al. 2018). Three zirconium precursors were used to synthesise three SO<sub>4</sub><sup>2-</sup>/ZrO<sub>2</sub> catalysts: (i) a SO<sub>4</sub><sup>2-</sup>/ZrO<sub>2sol-gel</sub> catalyst was prepared using the Zr(OCH<sub>2</sub>CH<sub>2</sub>CH<sub>3</sub>)<sub>4</sub> precursor. Zr(OCH<sub>2</sub>CH<sub>2</sub>CH<sub>3</sub>)<sub>4</sub> (5 mL) was first mixed with 6.6 mL of 1-propanol. Subsequently, 9.7 mL of 0.5 M aqueous H<sub>2</sub>SO<sub>4</sub> was added dropwise into the prepared mixed solution and was stirred vigorously at ambient temperature for 6 h. The formed gels were filtered, dried at 100 °C for overnight and were calcined at 625 °C for 4 h. (ii) A SO<sub>4</sub><sup>2-</sup>/ZrO<sub>2precipitation</sub> catalyst was prepared through precipitation using the ZrOCl<sub>2</sub>·8H<sub>2</sub>O precursor. About 21 mL aliquot of the 1 M NaOH solution was added slowly into 5 mL of ZrOCl<sub>2</sub>·8H<sub>2</sub>O under mild stirring at ambient temperature until pH 8 was reached. The formed catalyst was washed thoroughly with distilled water, filtered and then dried at 100 °C (12 h). Subsequently, 5.2 g of prepared powder was mixed with 4.6 mL of 0.5 M H<sub>2</sub>SO<sub>4</sub> at room temperature and stirred overnight. The final form SO<sub>4</sub><sup>2-</sup>/ZrO<sub>2</sub> was filtered, dried at 100 °C and then calcined at 625 °C for 4 h (Oh et al. 2013a). (iii) A SO<sub>4</sub><sup>2-</sup>/ZrO<sub>2commercial</sub> was synthesised by commercially available Zr(OH)<sub>4</sub>. Zr(OH)<sub>4</sub> (5.2 g) was mixed with 4.6 mL of 0.5 M H<sub>2</sub>SO<sub>4</sub> at room temperature and stirred overnight. The resulting SO<sub>4</sub><sup>2-</sup>/ZrO<sub>2</sub> catalyst was filtered, dried at 100 °C and then calcined at 625 °C for 4 h.

## Catalyst characterisations

The catalyst properties that focus on the texture were analysed using the N<sub>2</sub> physisorption method [BELSORP-max analyser (Japan)]. The samples were degassed for a period of 5 h under vacuum condition at a temperature of 200 °C. The sample particle size was measured using a Malvern MS3000 particle sizer (dry) with a working pressure of 2 bar. By using the water contact angle method of KRUSS DSA100, the different hydrophobicity levels of the catalyst were

measured. Acid–base titration method was used in determining catalyst acidity (mmol/g). Degassing of the catalyst sample was done at a temperature of 120 °C with a reaction time of 3 h. Following that, the sample is mixed in 25 mL of NaCl (2 M) and stirring was done at room temperature for about 24 h to attain equilibrium. Subsequently, the resultant was titrated with 8.38 × 10<sup>-3</sup> M of sodium hydroxide solution (Kong et al. 2018). The X-ray diffraction (XRD) patterns of the catalysts were recorded with a Bruker D8 Da Vinci diffractometer in Bragg–Brentano configuration by using Cu K Alpha 1,2 radiation (λ = 1.54056 Å) over the 2θ range of 10°–80°. Fourier-transform infrared (FTIR) spectra were performed using a PerkinElmer, Spectrum BXII spectrometer ranging from 200 to 4000 cm<sup>-1</sup> to identify functional groups on the catalyst surface. A field-emission scanning electron microscope (Model JSM-7100F) was used to analyse the surface morphology of the catalyst at an acceleration voltage of 1–30 kV. Thermogravimetric analysis was conducted to determine the catalyst thermal stability by applying the Mettler Toledo model at a rate of 10 °C/min and operating temperature from 25 to 900 °C.

## Catalytic reaction

Using a batch reactor with a working volume of 250 mL, the catalytic esterification was accomplished. The equipment is connected with a temperature gauge, condenser and a vacuum system. The esterification process is performed at a temperature of 160 °C utilising an equimolar ratio of reactant and constant acidity (1.55 mmol H<sup>+</sup>) for 8 h. The analysis was performed utilising HPLC. The type of column and the solvent employed for this particular study can be found in our previous study (Kong et al. 2018). By using Eqs. (1)–(3), respectively, the conversion, yield and selectivity are calculated:

**Table 1** Textural properties of the different types of SO<sub>4</sub><sup>2-</sup>/ZrO<sub>2</sub> catalysts and ZrO<sub>2</sub>-SiO<sub>2</sub>-Me&Et-PhSO<sub>3</sub>H catalyst

Catalysts	BET			Acidity (mmol/g)	Particle size distribution <sup>c</sup> (µm)	Contact angle analysis <sup>d</sup> (degree)
	Area <sup>a</sup> (m <sup>2</sup> /g)	Pore volume <sup>b</sup> (cm <sup>3</sup> /g)	Average pore diameter (nm)			
ZrO <sub>2</sub> -SiO <sub>2</sub> -Me&Et-PhSO <sub>3</sub> H	79.75	0.0247	3.77	0.62	5.01	41.5
SO <sub>4</sub> <sup>2-</sup> /ZrO <sub>2</sub> sol-gel	85.29	0.475	4.85	0.61	11.3	9.0
SO <sub>4</sub> <sup>2-</sup> /ZrO <sub>2</sub> precipitation	44.91	0.079	3.77	0.35	4.36	12.1
SO <sub>4</sub> <sup>2-</sup> /ZrO <sub>2</sub> commercial	60.06	0.240	3.77	0.44	12.5	10.8

<sup>a</sup>Total surface area was calculated using Brunauer–Emmett–Teller (BET) equation

<sup>b</sup>Barrett–Joyner–Halenda (BJH) method was employed in determining pore volume and average pore diameter

<sup>c</sup>Particle size distribution of catalyst was measured by Malvern particle sizer

<sup>d</sup>Contact angle analysis was employed for measuring catalyst hydrophobicity

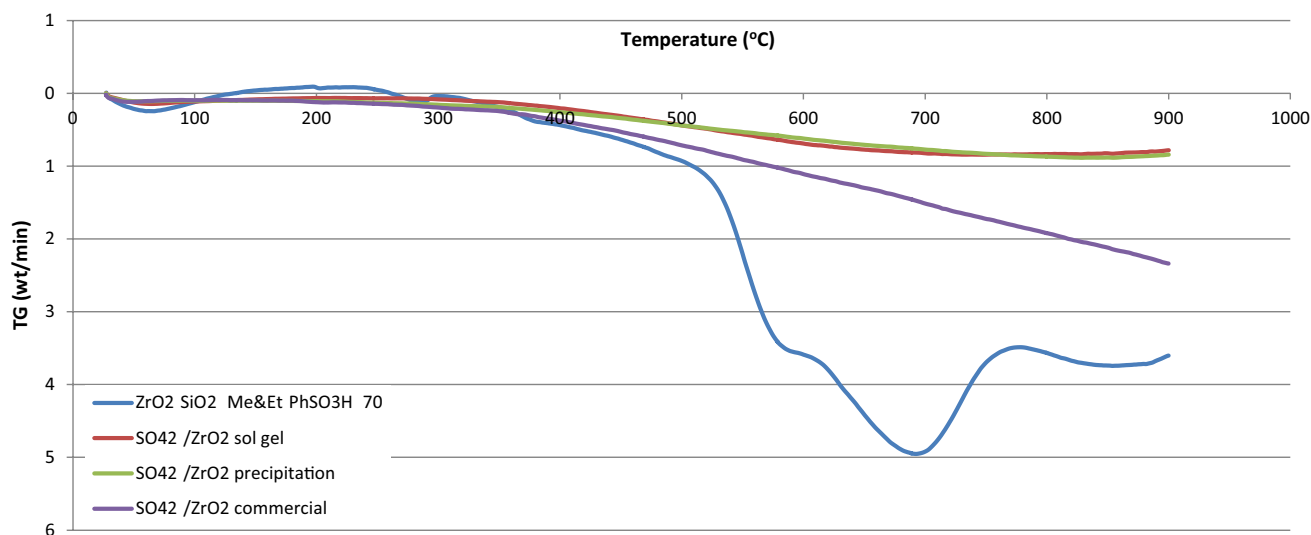


**Fig. 1** TGA curves for **a**  $\text{ZrO}_2\text{-SiO}_2\text{-Me\&Et-PhSO}_3\text{H}$  **b**  $\text{SO}_4^{2-}/\text{ZrO}_2$  sol-gel **c**  $\text{SO}_4^{2-}/\text{ZrO}_2$  precipitation **d**  $\text{SO}_4^{2-}/\text{ZrO}_2$  commercial

$$\text{Conversion (C)} = \frac{\text{mol}_{\text{OA}_{\text{consumed}}}}{\text{mol}_{\text{OA}_{\text{initial}}}} \times 100\% \quad (1)$$

$$\text{Yield}_{\text{total GMO,GDO,GTO}}(\text{Y}) = \frac{\text{mol}_{\text{total esters}}}{\text{mol}_{\text{OA}_{\text{initial}}}} \times 100\% \quad (2)$$

$$\text{Selectivity}_{\text{GMO}}(\text{S}) = \frac{\text{mol}_{\text{GMO}}}{\text{mol}_{\text{total GMO+GDO+GTO}}} \times 100\%. \quad (3)$$

## Results and discussion

### Catalyst characterisations

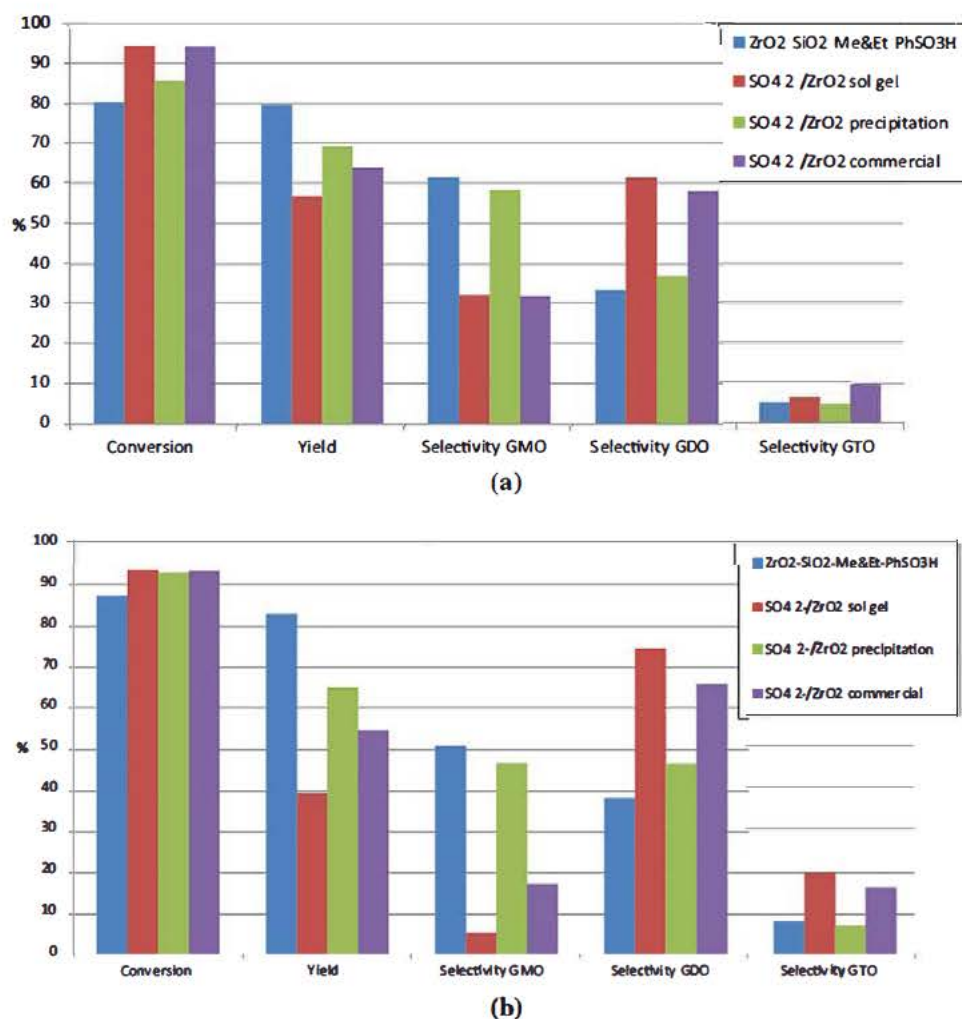
The synthesised catalyst ( $\text{ZrO}_2\text{-SiO}_2\text{-Me\&Et-PhSO}_3\text{H}$ ) and three  $\text{SO}_4^{2-}/\text{ZrO}_2$  catalysts were evaluated at a constant 1.55 mmol  $\text{H}^+$  catalyst acidity and identical reaction conditions (160 °C reaction temperature, an equimolar ratio of reactant and 8 h). Those optimal reaction conditions were obtained from the previous optimisation study (Kong et al. 2018). The textural properties and hydrophobicity of each catalyst are summarised in Table 1. The acidity of  $\text{SO}_4^{2-}/\text{ZrO}_2$  catalysts ranged from 0.35 mmol/g to 0.62 mmol/g. With regard to the influence of catalyst acidity on the reaction activity and selectivity, comparative studies were carried out at a constant concentration of 1.55 mmol  $\text{H}^+$  to investigate the effect of textural property on the reaction performance. As it was reported, factors affecting the total performance of catalysts such as the acidity of catalyst

should be eliminated, especially in studying the effect of complex catalyst structure (Ogino et al. 2018).

The surface areas of  $\text{SO}_4^{2-}/\text{ZrO}_2$  catalysts prepared using different precursors ( $\text{SO}_4^{2-}/\text{ZrO}_2$  sol-gel,  $\text{SO}_4^{2-}/\text{ZrO}_2$  precipitation and  $\text{SO}_4^{2-}/\text{ZrO}_2$  commercial) were 85, 44 and 60  $\text{m}^2/\text{g}$ , respectively. These results corresponded with those obtained by Oh et al. (Oh et al. 2013b). In addition, the hydrophobicity of each catalyst was examined. The results showed that all  $\text{SO}_4^{2-}/\text{ZrO}_2$  catalysts, regardless of the presence of Zr precursors, were less hydrophobic (as the obtained contact angle degree was low) compared with that of the designed catalyst  $\text{ZrO}_2\text{-SiO}_2\text{-Me\&Et-PhSO}_3\text{H}$ . The acidity level of  $\text{SO}_4^{2-}/\text{ZrO}_2$  sol-gel was identical with  $\text{ZrO}_2\text{-SiO}_2\text{-Me\&Et-PhSO}_3\text{H}$  (0.6 mmol/g), while  $\text{SO}_4^{2-}/\text{ZrO}_2$  commercial and  $\text{SO}_4^{2-}/\text{ZrO}_2$  precipitation demonstrated lower acidity level, 0.44 mmol/g and 0.35 mmol/g, respectively. FTIR spectra were employed to characterise and clarify the composition of the synthesised materials. For  $\text{ZrO}_2\text{-SiO}_2\text{-Me\&Et-PhSO}_3\text{H}$ , a visible band at 1061  $\text{cm}^{-1}$  was observed, which was ascribed to the elongating vibration of Si-O-Si, Si-O and Si-O-Zr bonds (Chen et al. 2016; Kong et al. 2018; Saravanan et al. 2016). Meanwhile, the bands at 988  $\text{cm}^{-1}$ , 1054  $\text{cm}^{-1}$ , 1125  $\text{cm}^{-1}$  and 1207  $\text{cm}^{-1}$  indicated the presence of sulphate group, for all types of  $\text{SO}_4^{2-}/\text{ZrO}_2$  catalysts (Chen et al. 2016; Saravanan et al. 2016).

The thermal stability of the catalysts was measured by TGA. The curves of  $\text{ZrO}_2\text{-SiO}_2\text{-Me\&Et-PhSO}_3\text{H}$  and different types of  $\text{SO}_4^{2-}/\text{ZrO}_2$  catalysts are displayed in Fig. 1. About 4 wt.% of mass loss was detected for  $\text{ZrO}_2\text{-SiO}_2\text{-Me\&Et-PhSO}_3\text{H}$  catalyst at the temperature ranging from 260 to 300 °C which attributed to the decomposition of sulphate moiety (Fang et al. 2015); nevertheless, at

**Fig. 2** Catalytic activities comparison of various Zr-based catalysts. Each reaction was performed at constant amount of 1.55 mmol  $H^+$ , equimolar ratio of OA and glycerol, 160 °C of reaction temperature and stirring speed of 650 rpm for 240 min (a) and 480 min (b)



560 °C–570 °C, a visible weight loss zone was observed for ZrO<sub>2</sub>-SiO<sub>2</sub>-Me&Et-PhSO<sub>3</sub>H due to SiO<sub>2</sub> material decomposition (Estevez et al. 2016). An intense weight loss peak at 700 °C was observed, and this might be due to the decomposition of Zr-Si. It could be explained that at high temperatures, an extensive surface dehydroxylation of the oxides occurred, with the breakdown of the porous oxide structure, whereas the thermal stability profile for SO<sub>4</sub><sup>2-</sup>/ZrO<sub>2</sub> sol-gel and SO<sub>4</sub><sup>2-</sup>/ZrO<sub>2</sub> precipitation is identical. They exhibit better thermal stability compared to SO<sub>4</sub><sup>2-</sup>/ZrO<sub>2</sub> commercial that may attribute to the species of Zr precursor used as the sulphonation and drying steps are similar for the three SO<sub>4</sub><sup>2-</sup>/ZrO<sub>2</sub> catalysts.

## Performance evaluation

Figure 2 shows the catalytic activity based on OA conversion, the yield of glycerol oleates and selectivity to GMO, GDO and GTO using ZrO<sub>2</sub>-SiO<sub>2</sub>-Me&Et-PhSO<sub>3</sub>H and various SO<sub>4</sub><sup>2-</sup>/ZrO<sub>2</sub> catalysts. Unlike ZrO<sub>2</sub>-SiO<sub>2</sub>-Me&Et-PhSO<sub>3</sub>H

catalyst, SO<sub>4</sub><sup>2-</sup>/ZrO<sub>2</sub> sol-gel-catalysed reaction produced considerably high conversion (93.0%) and high GDO selectivity (61.3%) at a rapid and brief processing time of 240 min (Fig. 2a), whereas further prolonging of the processing time to 480 min causes an increase in the GDO and GTO selectivity to approximately 75% and 20%, respectively (Fig. 2b). SO<sub>4</sub><sup>2-</sup>/ZrO<sub>2</sub> sol-gel catalyst produced the highest amount of GDO and GTO at an equimolar ratio of OA and glycerol at 160 °C. The obtained selectivity for SO<sub>4</sub><sup>2-</sup>/ZrO<sub>2</sub> precipitation ( $S_{GMO} = 59\%$  and  $S_{GDO} = 36\%$ ) was comparable to that of ZrO<sub>2</sub>-SiO<sub>2</sub>-Me&Et-PhSO<sub>3</sub>H ( $S_{GMO} = 61\%$  and  $S_{GDO} = 33\%$ ) at 240 min. A longer reaction time (480 min) for SO<sub>4</sub><sup>2-</sup>/ZrO<sub>2</sub> precipitation catalyst made it possible to obtain equal selectivity of GMO and GDO (both 46%). SO<sub>4</sub><sup>2-</sup>/ZrO<sub>2</sub> commercial achieved a high conversion profile and GDO selectivity at 480 min ( $C = 93\%$ ,  $S_{GMO} = 17\%$  and  $S_{GDO} = 66\%$ ), but its GDO selectivity was much lower than that of the SO<sub>4</sub><sup>2-</sup>/ZrO<sub>2</sub> sol-gel ( $S_{GDO} = 74.6\%$ ) at 480 min.

The resultant trends showed that the SO<sub>4</sub><sup>2-</sup>/ZrO<sub>2</sub> catalysts generally presented better conversions than that of ZrO<sub>2</sub>-SiO<sub>2</sub>-Me&Et-PhSO<sub>3</sub>H but with a much lower yield.



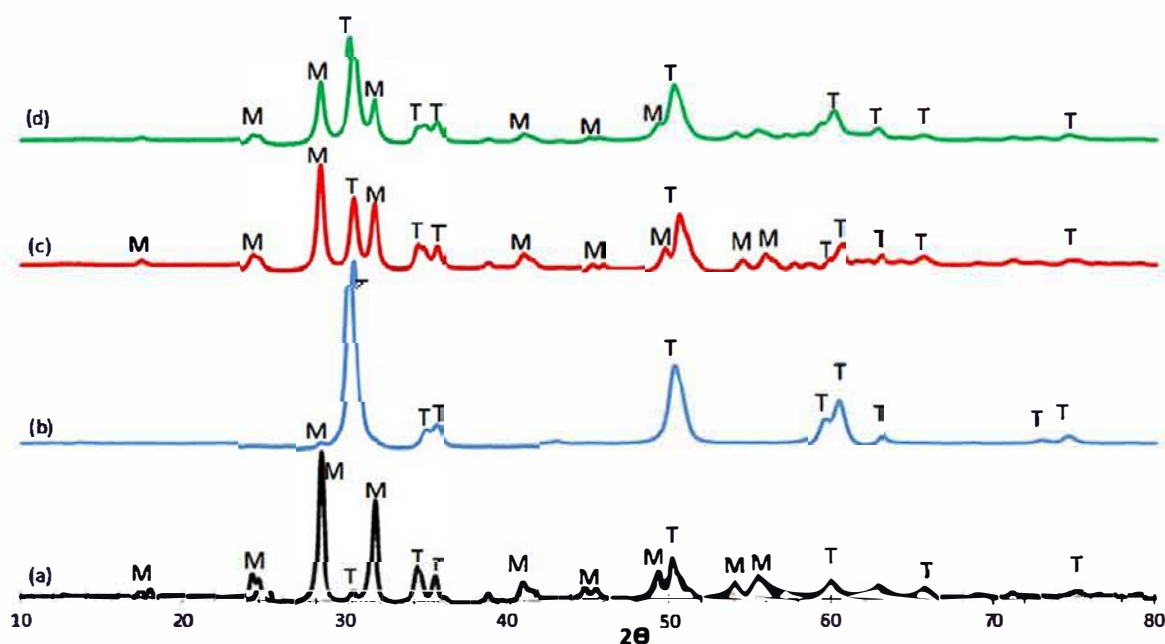
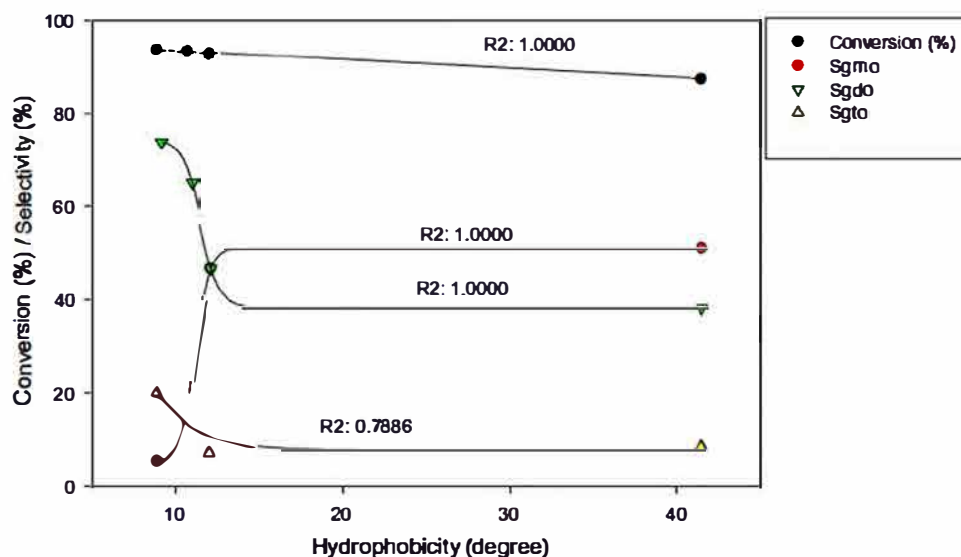


Fig. 3 XRD patterns of a  $\text{ZrO}_2\text{-SiO}_2\text{-Me\&Et-PhSO}_3\text{H}$ , b  $\text{SO}_4^{2-}/\text{ZrO}_2$  sol-gel, c  $\text{SO}_4^{2-}/\text{ZrO}_2$  precipitation and d  $\text{SO}_4^{2-}/\text{ZrO}_2$  commercial

Fig. 4 Correlation of pore volume with conversion and selectivity at 1.55 mmol  $\text{H}^+$  of controlled acidity and optimised operating conditions



The high conversion (94%) and low yield (39%) with selectivity favourable to GDO and GTO ( $S_{\text{GDO}} = 75\%$  and  $S_{\text{GTO}} = 20\%$ ) at 480 min for  $\text{SO}_4^{2-}/\text{ZrO}_2$  sol-gel-catalysed reaction, which is highly attributed to the catalyst's pore volume or high availability of active sites for the organic reactants (Kuwahara et al. 2014). The formation rates of the high molecular weight GDO and GTO were high for the catalyst with higher pore volume ( $\text{SO}_4^{2-}/\text{ZrO}_2$  sol-gel,  $0.475 \text{ cm}^3/\text{g}$ ) and ( $\text{SO}_4^{2-}/\text{ZrO}_2$  commercial,  $0.240 \text{ cm}^3/\text{g}$ ), which may subsequently lead to undesirable product formation. Remarkably, the role of catalyst hydrophobicity is effective in obtaining

a high product yield. Therefore, the correlation between the structure/property of catalysts and the catalytic performance was investigated in the following section. Understanding the correlation characteristics of catalyst to reaction is vital in developing effective catalysts (Diao et al. 2015).

### Correlation between $\text{SO}_4^{2-}/\text{ZrO}_2$ catalyst properties and selectivity/activities

Two correlations were successfully established. Firstly, the correlation between structural properties and selectivity

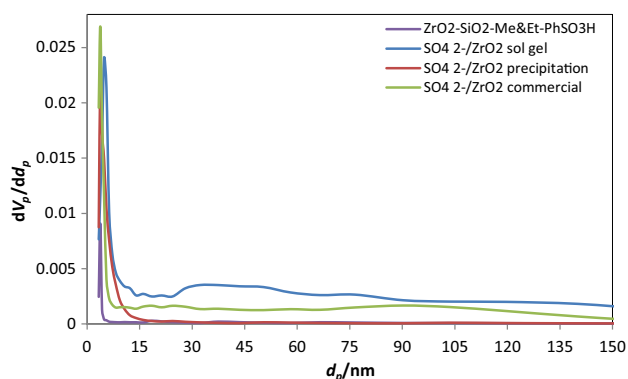


**Fig. 5** BJH plots of **a**  $\text{ZrO}_2\text{-SiO}_2\text{-Me\&Et-PhSO}_3\text{H}$ , **b**  $\text{SO}_4^{2-}/\text{ZrO}_2$  sol-gel, **c**  $\text{SO}_4^{2-}/\text{ZrO}_2$  precipitation and **d**  $\text{SO}_4^{2-}/\text{ZrO}_2$  commercial

was made. The correlation between textural properties and selectivity has been proven by XRD and BET results, whereby the finding showed that the thermodynamically stable monoclinic phase catalyst can contribute to smaller pore size; consequently, lower selectivity of the product can

be dominated in the product synthesis. In addition, the correlation of catalyst's hydrophobicity with selectivity/initial reaction rate was also proven. The higher hydrophobicity of catalyst leads to a higher initial rate, indicating that the initial reaction rate can be accelerated by the hydrophobicity surface of the catalyst.

### Correlation between structural properties and selectivity

Figure 3 demonstrates the XRD patterns for various catalysts. The XRD results indicated that  $\text{ZrO}_2\text{-SiO}_2\text{-Me\&Et-PhSO}_3\text{H}$  catalyst mainly comprises monoclinic phase and a minor tetragonal phase. A comparison of the XRD results of different types of  $\text{SO}_4^{2-}/\text{ZrO}_2$  catalysts with  $\text{ZrO}_2\text{-SiO}_2\text{-Me\&Et-PhSO}_3\text{H}$  can provide a correlation between the structural properties and the selectivity of the product mixture.

All  $\text{SO}_4^{2-}/\text{ZrO}_2$  catalysts possessed a highly tetragonal phase and less monoclinic phase. The acidic tetragonal phase may be stabilised by sulphated group (Oh et al. 2013b). XRD results also clearly revealed that

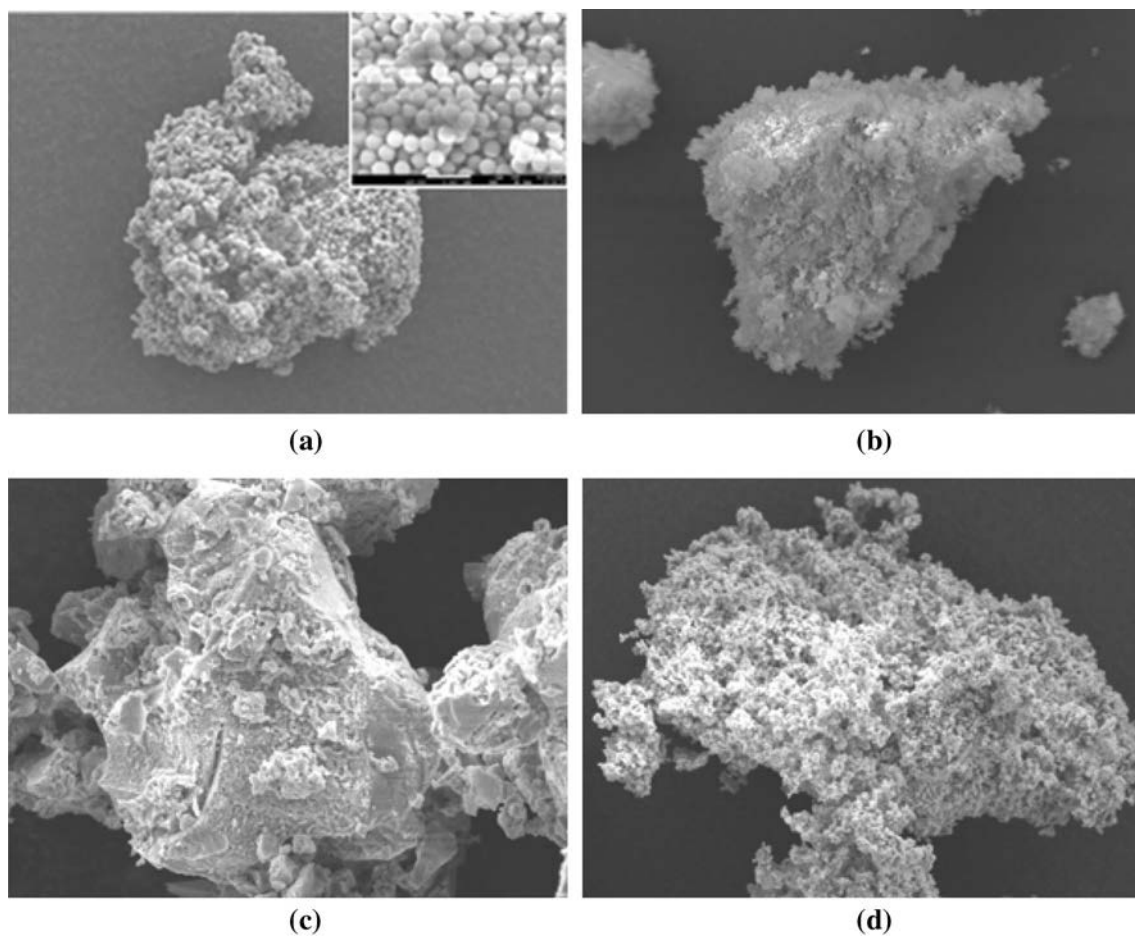


**Fig. 6** FESEM images for **a**  $\text{ZrO}_2\text{-SiO}_2\text{-Me\&Et-PhSO}_3\text{H}$ , **b**  $\text{SO}_4^{2-}/\text{ZrO}_2$  sol-gel, **c**  $\text{SO}_4^{2-}/\text{ZrO}_2$  precipitation, **d**  $\text{SO}_4^{2-}/\text{ZrO}_2$  commercial

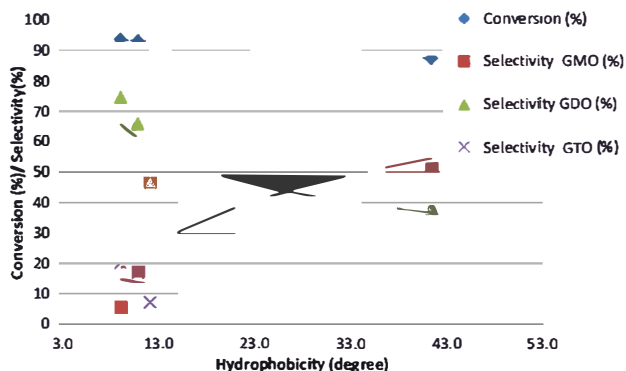


Fig. 7 Correlation between hydrophobicity and the conversion and selectivity at steady molar acidity of 1.55 mmol H<sup>+</sup> and operating parameters

Table 2 Turnover frequency of each catalyst during the first 15 min of reaction

Entry	Catalyst	TOF (h <sup>-1</sup> ) <sup>a</sup>
1	ZrO <sub>2</sub> -SiO <sub>2</sub> -Me&Et-PhSO <sub>3</sub> H	61.4
2	SO <sub>4</sub> <sup>2-</sup> /ZrO <sub>2</sub> sol-gel	48.7
3	SO <sub>4</sub> <sup>2-</sup> /ZrO <sub>2</sub> precipitation	47.9
4	SO <sub>4</sub> <sup>2-</sup> /ZrO <sub>2</sub> commercial	57.5

<sup>a</sup>Turnover frequency (TOF)= overall amount of moles converted into the anticipated product by one mole of active site in 15 min of reaction time

ZrO<sub>2</sub>-SiO<sub>2</sub>-Me&Et-PhSO<sub>3</sub>H catalyst was composed of a more thermodynamically stable monoclinic phase than the other SO<sub>4</sub><sup>2-</sup>/ZrO<sub>2</sub> catalysts. The monoclinic diffractions at 16°, 26°, 28° and 32° were more intense than those of SO<sub>4</sub><sup>2-</sup>/ZrO<sub>2</sub> precipitation (c) and SO<sub>4</sub><sup>2-</sup>/ZrO<sub>2</sub> commercial (d). Notably, no monoclinic peak was observed at SO<sub>4</sub><sup>2-</sup>/ZrO<sub>2</sub> sol-gel (b), but a crystalline tetragonal phase was mostly detected. This result reasonably corresponds with the highest pore volume (0.475 cm<sup>3</sup>/g) and pore size (4.85 nm) of SO<sub>4</sub><sup>2-</sup>/ZrO<sub>2</sub> sol-gel obtained in the BET results (refer to Table 1). The tetragonal phase was highly attributed to the different precursors used with identical calcination temperature and calcined time. Crystallinity was also proven to affect the type of zirconia precursor (Rashad and Baioumy 2008).

Consequently, the relationship between the textural properties of each catalyst is related to the selectivity and conversion obtained from the reaction. Figure 4 displays the correlation between pore volume versus conversion and selectivity. The experimental results fitted with the curve representing selectivity and conversion. This work proved the importance of pore volume in controlling product selectivity. Notably, increasing the pore volume of a catalyst can

increase the formation of GDO and GTO with large molecular sizes. Furthermore, GMO formation was unfavourable when catalysed by catalyst with a large pore volume. The conversion rate increased gradually with the increased catalyst pore volume.

The pore size (average pore diameter (nm); Table 1) was correlated with product selectivity, but the outcome was irrational because the obtained average pore diameter mostly ranged at the same peak (3.77 nm). Nevertheless, a remarkable phenomenon was observed in the BJH plot of different catalysts (Fig. 5). The high selectivity of GDO and GTO detected in the reaction mixtures using the SO<sub>4</sub><sup>2-</sup>/ZrO<sub>2</sub> sol-gel and SO<sub>4</sub><sup>2-</sup>/ZrO<sub>2</sub> commercial catalysts was attributed to their macroporous sizes, which exceeded 50 nm, and mesoporous catalyst (20–50 nm). Nonetheless, the pore sizes of ZrO<sub>2</sub>-SiO<sub>2</sub>-Me&Et-PhSO<sub>3</sub>H and SO<sub>4</sub><sup>2-</sup>/ZrO<sub>2</sub> precipitation were highly uniform and < 15 nm. The BJH plots of each catalyst clarified the influence of pore size on product selectivity.

The FESEM images for ZrO<sub>2</sub>-SiO<sub>2</sub>-Me&Et-PhSO<sub>3</sub>H, SO<sub>4</sub><sup>2-</sup>/ZrO<sub>2</sub> sol-gel, SO<sub>4</sub><sup>2-</sup>/ZrO<sub>2</sub> precipitation and SO<sub>4</sub><sup>2-</sup>/ZrO<sub>2</sub> commercial are presented in Fig. 6. ZrO<sub>2</sub>-SiO<sub>2</sub>-Me&Et-PhSO<sub>3</sub>H catalyst (Fig. 6a) demonstrates the formation of monodispersed spherical silica particles on zirconia support which resulted from TEOS hydrolysis and succeeding condensation (Kong et al. 2018; Rahman and Padavettan 2012). Unlike ZrO<sub>2</sub>-SiO<sub>2</sub>-Me&Et-PhSO<sub>3</sub>H, all SO<sub>4</sub><sup>2-</sup>/ZrO<sub>2</sub> catalysts presented typical rough and irregular surface morphology. It can be observed that SO<sub>4</sub><sup>2-</sup>/ZrO<sub>2</sub> precipitation exhibited rougher and higher pore space. Meanwhile, the crystallinity and morphology for SO<sub>4</sub><sup>2-</sup>/ZrO<sub>2</sub> sol-gel and SO<sub>4</sub><sup>2-</sup>/ZrO<sub>2</sub> commercial are almost identical. The morphology evidenced that the nature of the zirconium precursor influences the crystalline and porous structure of the catalyst.

### Correlation between hydrophobicity and selectivity/initial reaction rate

The correlation of catalyst hydrophobicity with the selectivity of reactions was evaluated. Figure 7 shows that the increase in hydrophobicity of the catalyst decreased the conversion rate. Linear regression with R-squared (*R*<sup>2</sup>) of 1.0 was obtained for conversion as a function of hydrophobicity. It is shown that increasing catalyst hydrophobicity causes a slight decrease in the conversion. In addition, good regression was obtained for selectivity of GMO, GDO and GTO using equation  $Y = y_0 + a(1 - e^{-bx})$ , which was obtained using Sigma Plot 11 software. The *R*<sup>2</sup> for GMO and GDO selectivity is 1 as experimental data are well fitted in the equation curve. It is shown that the selectivity for GMOs increased exponentially from 8 to 13 degrees of hydrophobicity value. Meanwhile, the selectivity of GDO decreased gradually by increasing the hydrophobicity of

the catalyst. In the case of the GTO selectivity, the  $R^2$  was lower (0.7886), but the trend clearly shows that the selectivity GTO decreased when the hydrophobicity value of catalyst was increased. It is similar to the finding of the previous work, and higher hydrophobicity of a catalyst's surface can reduce GTO formation selectivity, which is very beneficial for GMO and GDO production. Unlike the pore textural properties, the increased hydrophobicity enhanced the GMO formation. The GDO and GTO selectivity decreased with higher hydrophobicity. Despite the decreased hydrophobicity and the total conversion of reaction at 8 h, the initial reaction rate or turnover frequency, which was calculated during the first 15-min reaction, indicated that a catalyst with improved hydrophobicity displayed an increased turnover frequency value (Table 2). Surface hydrophobicity plays an important role in esterification reactions with polyols (glycerol) (Kotwal et al. 2013). The importance of the catalytic system is vital to enhance production on GMO and GDO due to its biphasic properties; it acts as important emulsifiers in the personal care and food industry. The increased selectivity of GTO resulted in poor dispersion of emulsion.

## Conclusions

This study proved that  $\text{ZrO}_2\text{-SiO}_2\text{-Me&Et-PhSO}_3\text{H}$  catalyst with a hydrophobic surface feature is a potential heterogeneous catalyst for glycerol esterification. In brief, the comparative study on  $\text{ZrO}_2\text{-SiO}_2\text{-Me&Et-PhSO}_3\text{H}$  with different  $\text{SO}_4^{2-}/\text{ZrO}_2$  catalysts validated the following points: (i) the structural crystallinity of  $\text{SO}_4^{2-}/\text{ZrO}_2$  is affected by the type of zirconia precursor and (ii) the importance of catalyst pore volume or high active sites accessibility for the organic reactants. The catalyst pore volume was correlated with the selectivity of the reaction; a large pore volume enabled the formation of large-molecular-size GDO and GTO. It is confirmed that highly uniform pores measuring  $< 5$  nm attained high GMO selectivity. In addition, this study has proven that the activity and selectivity of catalytic reactions are dependent on the catalyst properties such as pore volume and pore size, catalyst acidity and hydrophobicity. Nevertheless, this work proved that  $\text{ZrO}_2\text{-SiO}_2\text{-Me&Et-PhSO}_3\text{H}$  with consistent narrow pore volume ( $0.0247 \text{ cm}^3/\text{g}$ ) and the hydrophobic property is the potential acid catalyst for the production of GMO, whereas  $\text{SO}_4^{2-}/\text{ZrO}_2$  sol-gel is more suited for GDO production. This study has proven that designated catalysts with specific pore volume and hydrophobic characteristics can produce the increasingly important GMO and GDO lipids, particularly in the health care and wellness sector, in order to formulate potential vehicles of drugs and useful bioactive compound. The thermodynamics of the catalytic reaction and modelling of the correlation between structure

and selectivity of the product can be framed in the future context of the study.

**Acknowledgement** The authors acknowledge the financial support provided by INCREASE CNRS France and supported by the Fundamental Research Grant Scheme (Malaysia, FRGS/1/2019/STG05/UNIM/02/2). Dual PhD scholarship (University of Malaya) and French government scholarship (Embassy France of Kuala Lumpur) are gratefully acknowledged. The technical support and facilities from Laboratoire de Génie Chimique and Sime Darby Plantation Research Sdn. Bhd. are highly appreciated.

## References

- Åkerman CO, Gaber Y, Ghani NA, Lämsä M, Hatti-Kaul R (2011) Clean synthesis of biolubricants for low temperature applications using heterogeneous catalysts. *J Mol Catal B Enzym* 72(3):263–269
- Barauskas J, Misiunas A, Gunnarsson T, Tiberg F, Johnsson M (2006) “Sponge” nanoparticle dispersions in aqueous mixtures of diglycerol monooleate, glycerol dioleate, and polysorbate 80. *Langmuir* 22(14):6328–6334
- Chen J, Chen J, Zhang X, Gao J, Yang Q (2016) Efficient and stable PS- $\text{SO}_3\text{H}/\text{SiO}_2$  hollow nanospheres with tunable surface properties for acid catalyzed reactions. *Appl Catal A: Gen* 516:1–8
- Diao Y, He H, Yang P, Wang L, Zhang S (2015) Optimizing the structure of supported Pd catalyst for direct oxidative esterification of methacrolein with methanol. *Chem Eng Sci* 135:128–136
- Estevez R, López MI, Jiménez-Sanchidrián C, Luna D, Romero-Salguero FJ, Bautista FM (2016) Etherification of glycerol with tert-butyl alcohol over sulfonated hybrid silicas. *Appl Catal A: Gen* 526:155–163
- Fang W, Wang S, Liebens A, De Campo F, Xu H, Shen W, Clacens J-M (2015) Silica-immobilized Aquivion PFSA superacid: application to heterogeneous direct etherification of glycerol with n-butanol. *Catal Sci Technol* 5(8):3980–3990
- Frost and Sullivan Research Service (2014) World fatty esters markets (technical insights). Retrieved from <http://www.frost.com/prod/servlet/report-brochure.pag?id=D483-01-00-00-00>
- Gaudin P, Jacquot R, Marion P, Pouilloux Y, Jérôme F (2011) Acid-catalyzed etherification of glycerol with long-alkyl-chain alcohols. *Chemsuschem* 4(6):719–722
- Hamerski F, Corazza ML (2014) LDH-catalyzed esterification of lauric acid with glycerol in solvent-free system. *Appl Catal A: Gen* 475:242–248
- Hamerski F, Prado MA, da Silva VR, Voll FAP, Corazza ML (2016) Kinetics of layered double hydroxide catalyzed esterification of fatty acids with glycerol. *React Kinet Mech Catal* 117(1):253–268
- Jérôme F, Pouilloux Y, Barrault J (2008) Rational design of solid catalysts for the selective use of glycerol as a natural organic building block. *Chemsuschem* 1(7):586–613
- Karam A, De Oliveira Vigier K, Marinkovic S, Estrine B, Oldani C, Jérôme F (2017) High catalytic performance of aquivion PFSA, a reusable solid perfluorosulfonic acid polymer, in the biphasic glycosylation of glucose with fatty alcohols. *ACS Catal* 7(4):2990–2997
- Kong PS, Aroua MK, Daud WMAW (2015) Catalytic esterification of bioglycerol to value-added products. *Rev Chem Eng* 31(5):437–451
- Kong PS, Aroua MK, Daud WMAW (2016a) Conversion of crude and pure glycerol into derivatives: a feasibility evaluation. *Renew Sust Energy Rev* 63:533–555



- Kong PS, Aroua MK, Daud WMAW, Lee HV, Cognet P, Peres Y (2016b) Catalytic role of solid acid catalysts in glycerol acetylation for the production of bio-additives: a review. *RSC Adv* 6(73):68885–68905
- Kong PS, Cognet P, Pérès Y, Esvan J, Daud WMAW, Aroua MK (2018) Development of a novel hydrophobic  $\text{ZrO}_2\text{-SiO}_2$  based acid catalyst for catalytic esterification of glycerol with oleic acid. *Ind Eng Chem Res* 57(29):9386–9399
- Konwar LJ, Mäki-Arvela P, Kumar N, Mikkola J-P, Sarma AK, Deka D (2016) Selective esterification of fatty acids with glycerol to monoglycerides over  $\text{-SO}_3\text{H}$  functionalized carbon catalysts. *React Kinet Mech Catal* 119(1):121–138
- Kotwal M, Deshpande SS, Srinivas D (2011) Esterification of fatty acids with glycerol over Fe–Zn double-metal cyanide catalyst. *Catal Commun* 12(14):1302–1306
- Kotwal M, Kumar A, Darbha S (2013) Three-dimensional, mesoporous titanasilicates as catalysts for producing biodiesel and biolubricants. *J Mol Catal A: Chem* 377:65–73
- Kulkarni CV, Wachter W, Iglesias-Salto G, Engelskirchen S, Ahualli S (2011) Monoolein: a magic lipid? *Phys Chem Chem Phys* 13(8):3004–3021
- Kuwahara Y, Kaburagi W, Nemoto K, Fujitani T (2014) Esterification of levulinic acid with ethanol over sulfated Si-doped  $\text{ZrO}_2$  solid acid catalyst: study of the structure–activity relationships. *Appl Catal A: Gen* 476:186–196
- Macierzanka A, Szeląg H (2004) Esterification kinetics of glycerol with fatty acids in the presence of zinc carboxylates: preparation of modified acylglycerol emulsifiers. *Ind Eng Chem Res* 43(24):7744–7753
- Ogino I, Suzuki Y, Mukai SR (2018) Esterification of levulinic acid with ethanol catalyzed by sulfonated carbon catalysts: Promotional effects of additional functional groups. *Catal Today* 314:62–69. <https://doi.org/10.1016/j.cattod.2017.10.001>
- Oh J, Yang S, Kim C, Choi I, Kim JH, Lee H (2013a) Synthesis of biolubricants using sulfated zirconia catalysts. *Appl Catal A* 455:164–171
- Oh J, Yang S, Kim C, Choi I, Kim JH, Lee H (2013b) Synthesis of biolubricants using sulfated zirconia catalysts. *Appl Catal A: Gen* 455(Supplement C):164–171
- Quispe CAG, Coronado CJR, Carvalho JA Jr (2013) Glycerol: production, consumption, prices, characterization and new trends in combustion. *Renew Sust Energy Rev* 27:475–493
- Rahman IA, Padavettan V (2012) Synthesis of silica nanoparticles by sol-gel: size-dependent properties, surface modification, and applications in silica-polymer nanocomposites: a review. *J Nanomater* 2012:15
- Rashad MM, Baioumy HM (2008) Effect of thermal treatment on the crystal structure and morphology of zirconia nanopowders produced by three different routes. *J Mater Process Technol* 195(1–3):178–185
- Saravanan K, Tyagi B, Bajaj HC (2016) Esterification of stearic acid with methanol over mesoporous ordered sulfated  $\text{ZrO}_2\text{-SiO}_2$  mixed oxide aerogel catalyst. *J Porous Mater* 23:937–946
- Singh D, Patidar P, Ganesh A, Mahajani S (2013) Esterification of oleic acid with glycerol in the presence of supported zinc oxide as catalyst. *Ind Eng Chem Res* 52(42):14776–14786
- Thengumpillil NBK, Penumarthy V, Ayyagari AL (2002) Process for the preparation of a monoglyceride: U.S. Patents
- Wee LH, Lescouet T, Fritsch J, Bonino F, Rose M, Sui Z, Martens JA (2013) Synthesis of monoglycerides by esterification of oleic acid with glycerol in heterogeneous catalytic process using tin–organic framework catalyst. *Catal Lett* 143(4):356–363
- Zhang Z, Huang H, Ma X, Li G, Wang Y, Sun G, Li A (2017) Production of diacylglycerols by esterification of oleic acid with glycerol catalyzed by diatomite loaded  $\text{SO}_4^{2-}/\text{TiO}_2$ . *J Ind Eng Chem* 53:307–316